Sphingosine-1-phosphate receptor 3 regulates the transendothelial transport of HDL and LDL in opposite ways

Velagapudi, Srividya ; Wang, Dongdong ; Poti, Francesco ; Feuerborn, Renata ; Robert, Jérôme ; Schlumpf, Eveline ; Yalcinkaya, Mustafa ; Panteloglou, Grigorios ; Potapenko, Anton ; Simoni, Manuela ; Rohrer, Lucia ; Nofer, Jerzy-Roch ; von Eckardstein, Arnold

DOI: https://doi.org/10.1093/cvr/cvad183

Sphingosine-1-phosphate receptor 3 regulates the transendothelial transport of HDL and LDL in opposite ways

Srividya Velagapudi, PhD[1,], Dongdong Wang, PhD[1*], Francesco Poti, PhD[2,3,*], Renata Feuerborn PhD[4], Jerome Robert, PhD[1], Eveline Schlumpf M.Sc[1], Mustafa Yalcinkaya, PhD[1], Grigorios Panteloglou, PhD[1], Anton Potapenko, PhD[1], Manuela Simoni, MD, PhD[3], Lucia Rohrer, PhD[1], Jerzy-Roch Nofer, MD MBA [4,5 *], and Arnold von Eckardstein, MD[1,*, $]*

1. Institute of Clinical Chemistry, University of Zurich and University Hospital of Zurich, Switzerland
2. Department of Medicine and Surgery - Unit of Neurosciences, University of Parma, Parma, Italy
3. Department of Biomedical, Metabolic and Neural Sciences - Unit of Endocrinology, University of Modena and Reggio Emilia, Modena, Italy
4. Central Laboratory Facility, University Hospital of Münster, Germany
5. . Institute of Laboratory Medicine, Marien-Hospital Osnabrück, Niels-Stensen-Kliniken, Osnabrück,Germany

*: equal contribution

$: Corresponding author: Arnold von Eckardstein, MD, Institute of Clinical Chemistry, University Hospital of Zürich, Switzerland, Rämistrasse 100, CH-8091 Zürich, Switzerland

Short title: S1P3 and transendothelial lipoprotein transport

Word count main manuscript including title page, abstract, translational perspective, main text, acknowledgements, references and legends: 9520 words, 1 table, 7 figures, 1 graphical abstract

Supplementary material: 13 supplementary figures, 2 supplementary tables

Abstract (250 words)

Aims: The entry of lipoproteins from blood into the arterial wall is a rate-limiting step in atherosclerosis. It is controversial whether this happens by filtration or regulated transendothelial transport.

Because sphingosine-1-phosphate (S1P) preserves the endothelial barrier, we investigated *in vivo* and *in vitro*, whether S1P and its cognate S1P receptor 3 ($S1P_3$) regulate the transendothelial transport of lipoproteins.

Methods and Results: Compared to apoE-haploinsufficient mice (CTRL), apoE-haploinsufficient mice with additional endothelium specific knock-in of $S1P_3$ ($S1P_3$-iECKI) showed decreased transport of LDL and Evan's Blue but increased transport of HDL from blood into the peritoneal cave. After 30 weeks of high-fat diet feeding, $S1P_3$-iECKI mice had lower levels of non-HDL-cholesterol and less atherosclerosis than CTRL mice. *In vitro*, stimulation with an $S1P_3$ agonist increased the transport of ^{125}I-HDL but decreased the transport of ^{125}I-LDL through human aortic endothelial cells (HAECs). Conversely, inhibition or knock-down of $S1P_3$ decreased the transport of ^{125}I-HDL but increased the transport of ^{125}I-LDL. Silencing of *SCARB1* encoding scavenger receptor B1 (SR-BI) abrogated the stimulation of ^{125}I-HDL transport by the $S1P_3$ agonist. The transendothelial transport of ^{125}I-LDL was decreased by silencing of *SCARB1* or *ACVLR1* encoding activin-like kinase 1 but not by interference with LDLR. None of the three knock-downs prevented the stimulatory effect of $S1P_3$ inhibition on transendothelial ^{125}I-LDL transport.

Conclusion: $S1P_3$ regulates the transendothelial transport of HDL and LDL oppositely by SR-BI-dependent and SR-BI-independent mechanisms, respectively. This divergence supports a contention that lipoproteins pass the endothelial barrier by specifically regulated mechanisms rather than passive filtration.

Translational Perspective

The entry of lipoproteins from blood into the arterial wall is a rate-limiting step in atherosclerosis. It is controversial whether this happens by filtration or regulated transendothelial transport. The antagonistic effects of activated or inhibited sphingosine-1-phosphate receptor S1P3 on HDL and LDL through endothelial cells supports the hypothesis that transendothelial lipoprotein transport occurs by specific mechanisms and pathways. By inhibiting the transendothelial transport of pro-atherogenic LDL and promoting the transendothelial transport of potentially anti-atherogenic HDL, S1P 3 (but also S1P1) may play an important role in the pathogenesis of atherosclerosis and serve as an interesting target for protection against atherosclerosis.

Key words: endothelium, sphingosine-1-phosphate, HDL, LDL, SR-BI

Introduction

According to the nowadays widely accepted "response-to-injury" theory, the accumulation of low density lipoproteins (LDL) in the arterial wall plays a pivotal role in the initiation and pathogenesis of atherosclerosis [1,2]. Conversely, the removal of cholesterol from the intima by cholesterol efflux to high density lipoproteins (HDL) and subsequent reverse cholesterol transport should confer protection against atherosclerosis[3]. Two principal determinants define the accumulation of lipoproteins within the arterial wall: first, the concentration of lipoproteins in plasma which has been intensively investigated and successfully exploited to develop drugs which also prevent the incidence of cardiovascular events[1]; second, the entering and leaving of the arterial wall by LDL and HDL through mechanisms that have yet remained elusive [2–4]. To reach the subendothelial space, both LDL and HDL must cross the intact endothelium. Traditionally, this transit is explained by passive filtration [4,5] although as early as in the 1980ies ultramicroscopic studies in rabbits indicated that aortic endothelial cells internalize and re-secrete LDL[6]. The paradigm of passive filtration has also been challenged by the identification of several rate-limiting factors of transendothelial lipoprotein transport, namely scavenger receptor SR-BI, activin-like kinase 1 (ACVRL1), as well as caveolin-1 for LDL[7–10] and SR-BI, ATP binding cassette transporter G1, endothelial lipase, and the ecto-ATPase/P2Y-receptor axis for HDL [11–13]. Moreover, SR-BI was found to regulate the removal of HDL from extravascular tissues, including the arterial wall, into lymphatic vessels [14,15].

Sphingosine-1-phosphate (S1P) is an endogenous lipid agonist of five G-protein coupled receptors termed $S1P_1$, $S1P_2$, $S1P_3$, $S1P_4$ and $S1P_5$ [16]. In the endothelium, binding of S1P to the $S1P_1$ or $S1P_3$ receptors promotes the closure of intercellular junctions and hence the maintenance of the endothelial barrier [17,18]. In parallel with reducing paracellular filtration of albumin, S1P was reported to increase the transcytosis of albumin through pulmonary microvascular endothelial cells[20]. In this way S1P controls the trafficking of solutes, proteins, and cells between intra- and extravascular compartments [18,19]. In mice, the knock-out of the S1P-binding protein apolipoprotein M (apoM)

caused a strong decrease of S1P levels in plasma and HDL as well as increases in the permeability of lung capillaries and the blood brain barrier for albumin suggesting the involvement of this compound in the transendothelial transport regulation [20–22]. We previously demonstrated that apolipoprotein (apo)M and the $S1P_1$ receptor promote rather than inhibit the transendothelial transport of HDL [23]. We show here that the $S1P_3$ receptor regulates the transendothelial transport of LDL and HDL in opposite directions both *in vitro* and *in vivo*.

Materials and Methods

Mouse models

Triple transgenic mice overexpressing murine $S1P_3$ exclusively in endothelial cells were developed by crossing two lines. The *S1pr3* $^{LoxP\text{-}STOP\text{-}LoxP\ (LSL)}$ line, generated by genOway (Lyon, France) using their patented Rosa26 locus Quick knock-in™ technology, carries a transgenic cassette in the Rosa26 locus, which harbors the *S1pr3* cDNA. It is separated from the synthetic cytomegalovirus early enhancer/chicken β-actin (*CAG*) strong promoter by a *LoxP-STOP-LoxP (LSL)* insert (Supplementary Figure 1). *S1pr3*^{LSL} mice were crossed to *Apoe*$^{-/-}$*Cdh5-CreER*^{T2} mice as described previously for *S1pr1*^{LSL} mice[23] so that the *S1pr3* transcript is expressed exclusively in the endothelial cell lineage. We term these $S1P_3$-inducible endothelial cell knock-in mice $S1P_3$-iECKI mice. Double heterozygous *Apoe*$^{+/-}$*Cdh5-CreER*^{T2} $^{+/-}$ mice were used as controls (CTRL). Genotyping was performed by classical PCR on DNA isolated from tail biopsies using the following primer sequences to identify the Cre-excised allele: For CATCAGGTTCTCCAAGACGATGAAGC; Rev AGCCTCTGCTAACCATGTTCATGCC (amplicon: 424 bp). The experiments on transport of lipoproteins and Evan's Blue as well as en face immunostaining of $S1P_3$ and SR-BI were performed on 10-12 weeks old female mice fed a regular chow diet. For atherosclerosis studies, following induction of $S1P_3$ overexpression, 6-week-old female mice received high-fat atherogenic diet (w/w:

1.25% cholesterol; 16% fat; 0,5% sodium cholate; Altromin, Lage, Germany; corresponding to Research Diets D12109) for 30 weeks. For euthanasia, animals were anaesthetized with 5% (v/v) isoflurane introduced via a vaporizer and then subjected to cervical dislocation. All experiments conformed to the guidelines from directive 2010/63/EU and were approved by the local animal protection authorities (LANUV, Recklinghausen, Germany, permit 84-02.04.2011.A351).

Immunostaining of aorta and quantification of atherosclerotic lesions

For immunostaining of $S1P_3$ and SR-BI in the aortic endothelium as well as quantification of atherosclerosis we proceeded as described previously[23]. For the immunostaining we used the anti-$S1P_3$ and anti-SRBI antibodies from Novus Biologicals (NBP2-24762 and NB400-101, respectively) at concentrations of 20 µg/ml and secondary antibodies from Novus Biologicals (NBP1-76096 or NBP1-72973) at concentrations of 3.3 µg/ml.

Lipoprotein Isolation and labeling

LDL (1.019<d<1.063 g/mL) and HDL (1.063<d<1.21 g/mL) were isolated from fresh human normolipidemic plasma by sequential ultracentrifugation as described previously[24,25]. LDL and HDL were radioiodinated with $Na^{125}I$ by the McFarlane monochloride procedure modified for lipoproteins [25]. Specific activities between 300-900 cpm/ ng of protein were obtained. For assessment of vascular permeability of lipoprotein in mice, LDL and HDL were labeled with DyLight™ 550 fluorescent dye (DyL, Thermo Fischer, Schwerte, Germany) according to the manufacturer's instruction and as described previously[23].

Assessment of vascular permeability for lipoproteins and Evans Blue

As described previously[23], Evans Blue (600 µg/animal), DyL-LDL or DyL-HDL (each 500 µg/animal) were injected in the tail vein of in $S1P_3$-iECKI, and CTRL mice 15 minutes prior to the *i.p.* injection of LPS (25 µg/animal). Mice were sacrificed after 3 h and their peritoneal cavities were washed with 10 mL of ice-cold heparinized PBS. The cells were spun down and the supernatants

were analyzed for Evans Blue with photometry (620 nm, FluoStar Optima, BMG LabTech, Ortenberg, Germany) and for DyL-LDL or DyL-HDL with fluorescence spectrometry (560 nm/590 nm, FluoStar Optima).

Cell culture

Human aortic endothelial cells (HAECs) from Cell Applications Inc (304-05a) were cultured in endothelial cell basal medium (LONZA Clonetics CC-3156 or ATCC PCS-100-030) with 5% fetal bovine serum (GIBCO), 100 U/mL of penicillin and 100 µg/mL streptomycin (Sigma-Aldrich), supplemented with singleQuots (LONZA Clonetics CC-4176 or ATCC PCS-100-041, containing hFGF, hVEGF, hIGF-1, hEGF, hydrocortisone, ascorbic acid, heparin) at 37ºC in a humidified 5% CO_2, 95% air incubator.

Small Interfering RNA Transfection

Endothelial cells were reverse transfected with small interfering RNA (Ambion silencer select, Life technologies) targeted to $S1P_3$ (cat. No. s4455, s4453), SR-BI (cat. No. s2648, s2649, s2650) or LDLR (cat. No. s224006, s224007, s4) or ACVRL1 (cat. No. s986, s988) and non-silencing control (cat. No. 4390843) at a final concentration of 5 nmol/L using Lipofectamine RNAiMAX transfection reagent (Invitrogen, 13778150) in an antibiotic-free medium. All experiments were performed 72 hours post-transfection and efficiency of transfection was confirmed with at least two siRNAs against each gene using quantitative RT-PCR and Western blotting.

Quantitative real time PCR

Total RNA was isolated using TRI reagent (Sigma T9424) according to the manufacturer's instruction. Genomic DNA was removed by digestion using DNase (Roche) and RNase inhibitor (Ribolock, Thermo Scientific). Reverse transcription was performed using M-MLVRT (Invitrogen, 200 U/µL) following the standard protocol as described by the manufacturer. Quantitative PCR was

done with Lightcycler FastStart DNA Master SYBR Green I (Roche) using gene specific primers as followed: *S1PR3* (For: TGA TCG GGA TGT GCT GGC; Rev: GAG TAG AGG GGC AGG ATG GTA), *SCARB1* (For: CTG TGG GTG AGA TCA TGT GG; Rev: GCC AGA AGT CAA CCT TGC TC), *LDLR* (For: AAGGACACAGCACACAACCA; Rev: CATTTCCTCTGCCAGCAACG), *ACVRL1* (For: CGA CTT CAA GAG CCG CAA TG; Rev: AGG ACT CAA AGC AGT CCG TG), normalized to *GAPDH* (For: CCC ATG TTC GTC ATG GGT GT; Rev: TGG TCA TGA GTC CTT CCA CGA TA).

Lipoprotein Binding, Cell association and Transport

The methods for the quantification of binding, association and transport of radiolabeled HDL and LDL by endothelial cells have been previously described [23]. Briefly, all assays were performed in DMEM (Sigma) containing 25 mmol/L HEPES and 0.2% BSA instead of FBS. Where indicated, cells were pretreated for 30 minutes at 37 ºC with either $S1P_3$ agonist CYM-5541 (Cat No: SML0680, Sigma, 100 nM) or $S1P_3$ inhibitor TY52156 (Cat No:2404, Axon Medchem, 110 nM). Following the pharmacological drug treatments, the cells were incubated with 10 µg/mL of ^{125}I-HDL or ^{125}I-LDL without (total) or with 40 times excess of non-labeled HDL/ LDL (unspecific) for 1 hour at 4 ºC for cellular binding and at 37ºC for association experiments. Specific cellular binding and association were calculated by subtracting the values obtained in the presence of excess unlabeled HDL/ LDL (unspecific) from those obtained in the absence of unlabeled HDL/ LDL (total).

Inulin permeability

HAECs were cultured on trans-well inserts for 72 hours and cells were later treated with indicated pharmacological drug inhibitors as indicated for 30 minutes. Post-treatments, cells in the apical compartment were incubated with 2 mCi/mL of ^{3}H-inulin, and the filtrated radioactivity was collected in the basolateral compartment after 1 hour [13].

Western Blotting

Endothelial cells were lysed in RIPA buffer (10 mmol/L Tris pH 7.4, 150 mmol/L NaCl, 1% NP-40, 1% sodium deoxycholate, 0.1% SDS, with protease and phosphatase inhibitors (complete EDTA (Roche)). 30 µg of protein (quantified with the micro BCA protein assay kit Cat No: 23245 from Thermo Scientific) were separated on SDS-PAGE and trans-blotted onto PVDF membranes (GE Healthcare). Membranes were blocked in PBS-T supplemented with 5% milk or BSA and incubated either for 1 hour at room temperature or overnight on shaker at 4 ºC with primary antibodies against S1P3 (ab108370, Abcam), SR-BI (NB400-131, Novus), LDLR (ab52818, Abcam), or ALK1 (ab108207, Abcam), at a dilution of 1:1000 in the same blocking buffer. Membranes were incubated for 1 hour at room temperature with HRP-conjugated secondary antibody (Dako) in blocking buffer at a dilution of 1:2500. Membranes were further incubated with chemiluminescence substrate for 1 minute (Pierce ECL plus, Thermo scientific) and imaged using Fusion Fx (Vilber). As the loading control TATA binding protein (TBP) was immunodetected with primary antibody at 1:5000 (ab51841, Abcam) and secondary antibody at 1:10000 dilutions.

Cell surface expression analysis of SR-BI and LDLR

Intact cells were biotinylated using 20 mg/mL EZ-Link sulfo-NHS-S-S-Biotin (Thermo Scientific) on ice with mild shaking. After 1 hour, biotin was quenched with ice-cold 50 mM Tris pH 7.4. Cells were lysed in RIPA buffer (total cell lysate) and 200-500 µg of lysates were incubated with 20 µL of BSA-blocked streptavidin beads suspension (GE Healthcare) for 16 hours at 4ºC and pelleted by centrifugation; the pellet represents surface proteins. Proteins were dissociated from the pellet by boiling with SDS loading buffer containing 50 mM of DTT and analyzed by SDS-PAGE and immunoblotted with SR-BI antibody (NB400-131, Novus), LDLR (ab52818, Abcam) and TBP (ab51841, Abcam).

FACS-based analysis of LDLR cell surface expression

Cell surface levels of LDLR were determined by flow cytometry. 72 hours after transfection, the medium was removed, the cells were washed twice with PBS and detached using Accutase (Sigma-Aldrich, A6964) for 5 minutes at 37°C. The cells were then collected using FACS buffer (PBS containing 0.5% BSA and 0.05% NaN_3), washed with ice cold FACS buffer and then incubated with Blocking Buffer (PBS containing 0.5% BSA and 2% FBS) for 1 hour on ice. After blocking, the cells were incubated with the monoclonal anti-LDLR antibody, LDLR (Progen, cat. number 61087) diluted 1:25 in FACS buffer for 1 hour on ice. After washing with FACS buffer, the cells were incubated with goat anti-mouse IgG (H+L) Cross-Adsorbed AlexaFluor 647-conjugated secondary antibody (Thermo Fischer Scientific cat. A-21236) diluted to a final concentration of 4 ug/ml in FACS buffer for 1 hour on ice in the dark. Finally, prior to acquisition, the cells were washed with FACS buffer and resuspended in ice cold FACS buffer containing Propidium Iodide (PI) to a final concentration of 1 ug/ml. Cells incubated with the secondary antibody only were used as negative controls to determine the signal-to-noise ratio. Sample acquisition was carried out on a BD LSR II Fortessa (BD-Biosciences) and using BD FACSDIVA™ software. Data analysis was carried out using FlowJo version 10 (FlowJO LLC,). Approximately 10^4 events per condition recorded at the final gate (PI negative) were used for analysis.

Statistical Analysis

The data sets for all validation experiments were analyzed using the GraphPad Prism 5 software. The individual values (technical replicates) obtained in the control group from each experimental run were averaged and the average was set to 100%. Further, the percentage difference of each individual technical replicate (of control group and other treatment conditions) was calculated with respect to the average value of the control group (which was set to 100%). Comparison between the means of two or multiple groups were performed with two-tailed Student's *t*-test and one-way analysis of variance for independent samples, respectively. Pairwise comparisons were performed

thereafter with Student-Newman-Keuls post hoc test. The data was obtained from at least three independent experiments, performed in triplicates or quadruplets. Values are expressed as mean±SEM. P<0.05 was regarded as significant.

Results

Endothelial overexpression of $S1P_3$ differentially regulates endothelial permeability for LDL, HDL, and Evans Blue in mice

To investigate the impact of the G-protein coupled receptor $S1P_3$ on transendothelial lipoprotein transport *in vivo*, we generated *Apoe* haploinsufficient mice which overexpress the human $S1P_3$ receptor ($S1P_3$-iECKI) under the control of a tamoxifen-inducible VE-cadherin promoter in endothelial cells only. Double heterozygous *Apoe*$^{+/-}$*Cdh5-CreER*$^{T2+/-}$ littermates were used as controls and comparators (hereafter termed CTRL) (Figure 1a). The successful knock-in and the increased expression of $S1P_3$ were demonstrated by genotyping (Figure 1b) and immunofluorescence microscopy of aortas, respectively (Figure 1c-f and Supplementary Figure 1a, b). Compared to CTRL mice (Figure 1c, d), the immunoreactivity for $S1P_3$ was much enhanced in aortas of $S1P_3$-iECKI mice (Figure 1e, f). Upon feeding with chow diet, plasma levels of cholesterol and triglycerides did not differ between $S1P_3$-iECKI mice (1.29 +/- 0.46 mmol/L and 0.78 +/- 0.17, N = 6) and control mice (1.05 +/- 0.19 mmol/L and 0.65 +/- 0.07 mmol/L, N = 4). Upon gel filtration, no major difference in the distribution of cholesterol and triglycerides among lipoproteins was seen (not shown). After 30 weeks of feeding a 1.25% cholesterol-containing Western diet, the $S1P_3$-iECKI mice had significantly lower levels of non-HDL-cholesterol and significantly higher levels of HDL-cholesterol as well as 60% less fatty lesions in their sinus aortae than Apoe-haploinsufficient CTRL mice (Supplementary Figure 2).

To assess the vascular permeability for albumin and lipoproteins in 10 - 12 weeks old female $S1P_3$-iECKI or CTRL mice fed a regular chow diet (5 or 6 per group) received intravenous injections of the albumin marker Evans Blue, DyL-LDL, or DyL-HDL 15 minutes prior to the *i.p* injection of LPS. $S1P_3$-iECKI mice differed significantly from CTRL mice by 49% less uptake of DyL-LDL and 49% more uptake of DyL-HDL into the peritoneal cave (all $P < 0.05$). The 15% decrease in Evans Blue uptake was not statistically significant (Table 1). We also tested if the experiment can be performed in the absence of LPS, but we did not recover any fluorescence of DyL-LDL or DyL-HDL beyond background, if no LPS was injected i.p.(Supplementary Table 1).

$S1P_3$ exerts opposite effect on the transendothelial transport of HDL and LDL through human aortic endothelial cells

We next investigated whether $S1P_3$ also regulates the transport of HDL and LDL through cultivated HAECs. First, we confirmed on both the mRNA and protein level the expression of $S1P_3$ (Supplementary Figure 3). Previous RNA sequencing studies recorded mRNA of $S1P_3$ in HAECs at levels that in average are lower than those of $S1P_1$ but much higher than those of $S1P_2$, $S1P_4$, or $S1P_5$ which were almost undetectable (Supplementary table 2) [26–29]. Similarly, to the *in vivo* data, activation of $S1P_3$ with the agonist CYM5541 at its IC50 concentration of 100 nM (Supplementary Figure 4), increased the transport of ^{125}I-HDL (Figure 2a) but decreased the transport of ^{125}I-LDL (Figure 2b). We then investigated whether these effects resulted from corresponding differences in the binding or uptake of the lipoproteins. Upon 30 minutes treatment of HAEC with 100 nM of CYM5541 at 37°C, specific cell association of HDL and LDL, which represents the combination of binding and uptake, was increased to 166% and reduced to 47%, respectively (Figures 2c and 2d). At 4°C the specific cellular binding of ^{125}I-HDL and ^{125}I-LDL was increased to 206% and decreased to 45%, respectively (Figures 2e and 2f)

We then determined how pharmacological or RNA inhibition of $S1P_3$ influence the endothelial interactions of radioiodinated HDL and LDL. At the IC50 concentration of 110 nM (Supplementary

Figure 5), the $S1P_3$ inhibitor TY52156 did not interfere with the permeability of ^{3}H-inulin (Supplementary Figure 6) through HAECs. TY52156 (110 nM) decreased the specific transport, association, and binding of ^{125}I-HDL to 56% (Figure 3a), 68%, (Figure 3b), and 51%, respectively, of the untreated control (Figure 3c). Conversely, transport, association, and binding + of ^{125}I-LDL were increased to 137% (Figure 3d), 136% (Figure 3e), and 141%, respectively (Figure 3f). RNA interference strongly reduced $S1P_3$ expression both on the mRNA (Supplementary Figure 3a) and protein level (Supplementary Figure 3b) without affecting $S1P_1$ expression (Supplementary Figure 3a, c) and decreased the cell association of ^{125}I-HDL by about 20% (Figure 4a) but increased the cell association of ^{125}I-LDL by about 40% (Figure 4b). Supporting the specificity of the $S1P_3$ agonist, the stimulatory effect of CYM5541 on the association of ^{125}I-HDL as well as its inhibitory effect on the association of ^{125}I-LDL were abrogated by silencing of $S1P_3$ (Figure 4a, b). Taken together, these results indicate that $S1P_3$ regulates endothelial cellular binding, association as well as transport of HDL and LDL into opposite directions.

$S1P_3$ regulates cellular binding, association and transendothelial transport of HDL via SR-BI

We previously reported that pharmacological activation of $S1P_1$ increases the transendothelial transport of HDL by promoting the translocation of SR-BI to the cell surface. In addition, SR-BI immunoreactivity was increased in the aorta of $S1P_1$ endothelial specific knock-in ($S1P_1$-iECKI) mice[23]. To determine whether $S1P_3$ also regulates trans-endothelial transport of HDL through involvement of SR-BI, we combined pharmacological activation of $S1P_3$ by CYM5541 with SR-BI silencing by siRNAs. The knockdown of SR-BI was efficient at the protein level (Supplementary Figure 7a). Silencing of SR-BI significantly decreased specific cellular binding, association, and transport by 40% (Figure 5a), 36% (Figure 5b), and 43% (Figure 5c), respectively. Activation of $S1P_3$ failed to stimulate the cellular binding, association, or transport of ^{125}I-HDL through endothelial cells when SR-BI was silenced (Figure 5). Cell surface biotinylation experiments showed that the activation of $S1P_3$ receptor increases the cell surface abundance of SR-BI (Figure 6a, b;

supplementary figure 8). The pharmacological inhibition of $S1P_3$ with TY52156 did not decrease the abundance of SR-BI on the cell surface (Figure 6a, b; supplementary figure 8). However, RNA interference against $S1P_3$ suppressed SR-BI expression both on the mRNA and protein level (Figures 6c, d; supplementary figure 9). RT-PCR of the distinct sequences revealed similar decreases of transcripts encoding SR-BI splice variants 1 and 2 (Supplementary Figure 10). Conversely, the knock-in of $S1P_3$ increased the protein abundance of SR-BI in the aortic endothelium of $S1P_3$ iECKi mice (Figure 6e and Supplementary Figure 11). Thus, $S1P_3$ appears to regulate SR-BI abundance by both fast posttranslational and sustained transcriptional mechanisms.

$S1P_3$ regulates transendothelial transport of LDL independently of LDLR, SR-BI, or ALK1

To identify the targets for the increased binding, association, and transport of ^{125}I-LDL upon $S1P_3$ inhibition (Figures 3d-f), we tested the involvement of receptors known to promote the uptake of LDL into endothelial cells, namely LDLR, SR-BI, and ACVRL1 [5,7,8] by using RNA interference. Recorded at the protein level, the knockdowns of *SCARB1 (*coding for SR-BI), *LDLR*, and *ACVRL1* (coding for ALK1) were efficient but also caused some off-target effects. SR-BI was abolished upon knock-down of *SCARB1* but increased upon knock-down of LDLR (Supplementary Figure 7a). LDLR protein was not detectable after knock-down of *LDLR* but increased upon knock-down of *SCARB1* or *ACVLR1* (Supplementary Figure 7b). ALK1 was abolished by knock-down of *ACVLR1* but also decreased upon silencing of *SCARB1* or *LDLR* (Supplementary Figure 7c). Silencing of *SCARB1 per se* decreased the cellular binding, association, and transport of ^{125}I-LDL by 34%, 36%, and 59%, respectively (Figure 7a-c). Also silencing of ACVRL1 *per se* decreased the cellular binding, association, and transport of ^{125}I-LDL by 64%, 59% and 65%, respectively (Figure 7a-c). However, the $S1P_3$ inhibitor continued to stimulate the binding, association, and transport of ^{125}I-LDL in the absence of either SR-BI or ALK1 (Figures 7 a, b and 7c).

Silencing LDLR *per se* significantly decreased specific cellular binding and association of ^{125}I-LDL by 54% and 68%, respectively (Figure 7a and b), but had no effect on the transport of ^{125}I-LDL (Figure 7c). In the absence of LDLR, the $S1P_3$ inhibitor failed to stimulate the cellular binding and association of ^{125}I-LDL (Figure 7a and b). Flow cytometry analysis did not reveal any change in the cell surface expression of LDLR either in response to drug treatment with the $S1P_3$-agonist or $S1P_3$-inhibitor or after RNA interference with $S1P_3$ (Supplementary Figure 12).

Taken together, these findings confirm that the transendothelial transport of LDL is limited by the abundance of SR-BI and ALK1 but not by LDLR. The data also indicate that $S1P_3$ inhibition stimulates transendothelial transport of ^{125}I-LDL independently of LDLR, SR-BI, or ALK1.

Discussion

It is controversial whether macromolecules including lipoproteins pass the endothelial barrier by active or passive transport. For a long time, the three-poremodel of Rippe and colleagues dominated the discussion [30]. It was most extensively investigated by the analysis of protein transport from the blood stream into the peritoneal fluid but extrapolated to microcirculation in general. The peritoneum consists of a layer of mesothelial cells that is covered by a basement membrane and a thicker layer of connective tissue. The latter also contains capillaries and lymphatics. The endothelial cells of the capillaries rather than the mesothelium or connective tissue limit the transport of macromolecules including proteins from the blood stream into the peritoneal cavity. The lymphatics are rather mediating the reverse transport out of the cavity back into the blood stream via the thoracic duct [31]. According to the three-pore-model, small pores with a diameter of 0.6 to 1.0 nm allow the passage of small molecules only, whereas large pores with a diameter of 40 to 60 nm allow the transport of large macromolecules (ie. also LDL with a Stokes diameter of 25 nm) without any restriction. Intermediate pores with a diameter of 8 to 12 nm would allow the transport of proteins with a Stokes

diameter below or within this threshold, for example albumin (6 nm) but also HDL (8-12 nm) [31]. Previous data on the regulation of endothelial barrier function by S1P also indicated rather unselective effects of S1P on transendothelial macromolecule transport by inducing the formation and maintenance of adherens and tight junctions [32] and, hence, did not contradict the three-pore model. Decreases of bioactive S1P plasma levels lead to the exudation of albumin into the extravascular space and to lung edema as well as increased permeability of the blood-brain barrier in apoM-knock-out animals [20–22]. Conversely, increases of S1P plasma levels in mice lacking sphingosine kinase 2 were reported to reduce the permeability of peritoneal capillaries for dextran beads and LDL [33].

In contrast to this classical model, our in *vivo* and *in vitro* experiments provide several pieces of evidence suggesting that the endothelial S1P-receptor $S1P_3$ differentially regulates the transendothelial transport of pro-atherogenic LDL and potentially anti-atherogenic HDL: On the one hand and in line with the general notion of S1P as a stabilizer of endothelial barriers, the endothelial overexpression of human $S1P_3$ in mice reduced the transendothelial transport of LDL and, less so, Evans Blue, a marker of albumin transport. Also, in accordance with an inhibitory role of S1P on transendothelial transport, the *in vitro* transendothelial transport by cultivated HAECs of LDL was decreased upon activation of $S1P_3$ but increased upon inhibition of $S1P_3$ by drugs or RNA interference with *S1P3*. On the other hand, and in contradiction to a general inhibitory effect of S1P on transendothelial macromolecule transport, the transendothelial transport of HDL was enhanced both *in vivo* and *in vitro* by the overexpression and activation, respectively, of $S1P_3$, and diminished upon inhibition of $S1P_3$. We previously reported similar opposing effects of $S1P_1$ on the transendothelial transport of HDL and albumin both *in vivo* and *in vitro* [23]. Like the $S1P_3$-iECKI mice described in this paper, $S1P_1$-iECKI mice with endothelium-specific knock-in of $S1P_1$ showed decreased atherosclerosis as well as LDL-and albumin transport but enhanced HDL transport into the peritoneum [23]. Likewise in cultivated HAECs, the binding, association and transendothelial transport

of HDL were enhanced by the $S1P_1$ agonist SEW2871 but decreased by the $S1P_1$ inhibitor W146 [23]. Conversely, the $S1P_1$ agonist and inhibitor suppressed and promoted, respectively, the binding, association, and transendothelial transport of LDL (Supplementary Figure 13). We postulate that the heterogeneous downstream responses account for differential effects of $S1P_3$ (and $S1P_1$) on the transport of HDL and LDL through endothelial cells. In view of the principally identical effects of $S1P_1$ and $S1P_3$ on the transendothelial transport of HDL on the one hand and albumin and LDL on the other hand, it is interesting to note that the loss or gain of function of the one receptor is not compensated or neutralized by the other neither by counter-regulated expression nor by function. Likewise, $S1P_1$ and $S1P_3$ did not mutually compensate the adverse effects of their knock-downs on nitric oxide production and apoptosis inhibition [31-33] It was even suggested that the two receptors cooperate at least upon interaction with S1P delivered by apoM containing HDL [34].

Interference with SR-BI abrogated the enhanced binding, uptake and transport of HDL elicited by the $S1P_3$-agonist. S1P-receptor activation appears to promote transendothelial HDL transport by a similar mechanism as the activation of $S1P_1$ by S1P [23] or VEGF receptor 2 by VEGF-A [35], namely by increasing the cell surface abundance of SR-BI. This may be due to the fact, that activation of either receptor induces Akt phosphorylation [36], which we previously found to mediate the stimulatory effect of VEGF on both SR-BI translocation and binding, uptake, and transport of HDL by HAECs [35]. In addition, sustained alterations of $S1P_3$ expression (but also $S1P_1$ expression) [23] either *in vivo* by knock-in or *in vitro* by RNA interference, change the total protein expression of SR-BI. The parallel decrease of *SCARB1* mRNA and SR-BI protein in HAECs treated with siRNA's against either $S1P_3$ or $S1P_1$ [23] suggests that this happens on the transcriptional level. The stimulatory effects of the $S1P_3$ (this paper) and $S1P_1$ agonists [23] on HDL transport were both prevented by RNA interference with *SCARB1* suggesting a causal link between the increase in SR-BI cell surface expression and increased HDL transport upon activation of these S1P receptors. However, the $S1P_3$ inhibitor reduced HDL transport without reducing the cell surface abundance of SR-BI. Although we cannot

rule out methodological limitations to assess any quantitative decrease in SR-BI cell surface abundance, one must also consider the possibility that $S1P_3$ inhibition interferes with additional proteins interacting with HDL and limiting its uptake and transport. In fact, by applying chemoproteomic ligand receptor capturing to the endothelial cell line EA.hy926, we recently found that HDL interacts with several cell surface proteins in the vicinity of SR-BI. Two of them are the TAM receptor family member MERTK and aminopeptidase N, whose knock-down also led to decreased HDL uptake into both EA-hy926 cells and HAECs [37,38]

Confirming data from other labs as well as our own lab, we found that SR-BI also mediates the binding, association, and transport of LDL by HAECs [8,10,39]. Therefore, it is surprising that the stimulation of $S1P_3$ rather inhibited transendothelial LDL transport (Figures 2d-f). The $S1P_1$ agonist SEW287 exerts the same effect (Supplementary Figure 13). By combining RNA interference with $S1P_3$ inhibition, we confirmed SR-BI as a limiting factor for transendothelial LDL transport but ruled out that it contributes to the enhanced transendothelial LDL transport upon inhibition of $S1P_3$ (Figure 7). Similarly, we previously showed in bovine aortic endothelial cells that VEGF promotes transendothelial transport of HDL in an SR-BI dependent manner but has no effect on LDL transport [35]. This discrepancy may be the result of different splice variants of SR-BI [39] expressed by endothelial cells. The two most prominent ones differ by the 45 carboxyterminal amino acid residues. Only variant 1 of SR-BI contains the binding sites for the adapter proteins PDZK1 and DOCK4 which were shown to be essential for cell surface expression in hepatocytes and endothelial LDL uptake, respectively [10,40]. However, siRNA interference with $S1P_3$ suppressed the two transcripts encoding SR-BI variants 1 and 2. It is therefore unlikely that differences in the regulation and function of the two splice variants of SR-BI explain the opposite effects of $S1P_3$ on the transendothelial transport of HDL and LDL. It is also important to note that SR-BI is no endocytic receptor per se [41]. Notably, in hepatocytes and steroidogenic cells, SR-BI binds both HDL and LDL, however without internalizing the entire particles. This suggests the contribution of endocytic co-

receptors that are present in endothelial cells but neither in hepatocytes nor steroidogenic cells. Our lab previously used chemoproteomic techniques to elucidate the surface proteome of endothelial cells and hepatocytes in general as well as specifically parts thereof that interact with HDL and anti-SR-BI antibodies. These analyses provided evidence of synapse-like many-to-many interactions between HDL and proteins of the cell surface. SR-BI is a core-protein in these interactions [37,38]. It may hence be that $S1P_3$ (and $S1P_1$) activate not only SR-BI but several other members of this HDL synapse. Vice versa, $S1P_3$ and $S1P_1$ may limit other members of an LDL-synapse and thereby overrule the effects of SR-BI on the uptake of LDL into a transcellular transport itinerary. As an alternative explanation, one may hypothesize that $S1P_3$ and $S1P_1$ activate an inhibitor of transendothelial LDL transport. By combining RNA interference with $S1P_3$ inhibition, we confirmed ACVRL1[7] as a limiting factor for transendothelial LDL transport but ruled out that it contributes to the enhanced transendothelial LDL transport upon $S1P_3$ inhibition. By RNA interference, we also showed the involvement of the LDL receptor in cellular binding and association of LDL. However, and in agreement with previous reports [7,42] silencing of LDLR did not interfere with the transendothelial transport of LDL. LDL-uptake via the LDL-receptor rather leads to lysosomal degradation rather than re-secretion of LDL [7,42]. Interestingly, interference with LDLR, prevented the stimulatory effect of $S1P_3$ inhibition on binding and association of LDL by HAECs. However, in contrast with the regulatory effect of $S1P_3$ on the cell surface expression of SR-BI, neither the activation, nor the inhibition nor the knock-down of $S1P_3$ altered the cell surface abundance of LDLR in HAECs (not shown). It thus appears that $S1P_3$ regulates endocytic LDLR functions. This may be an important regulatory step in the removal of S1P from the plasma as LDLR was suggested to bind apoM containing LDL and thereby contribute to S1P clearance [43]. However, neither LDLR nor ALK1 explain the opposite effects of $S1P_3$ and $S1P_1$ on the transendothelial transport of HDL and LDL.

In conclusion, we here showed that $S1P_3$ regulates the endothelial binding, uptake and transport of HDL and LDL in an antagonistic manner. By inhibiting the transendothelial transport of pro-atherogenic LDL and promoting the transendothelial transport of potentially anti-atherogenic HDL, $S1P_3$ may play an important role in the pathogenesis of atherosclerosis and serve as an interesting target for protection against atherosclerosis, following the example of the anti-ALK1 antibody which in a preclinical model reduced atherosclerosis by interfering with transendothelial LDL transport[44]. In fact, several animal studies showed that genetic or pharmacological interference with S1P generation and degradation by sphingosine kinase 2 [45,46] and S1P lyase [47], respectively, the S1P binding protein apoM [23,48], or S1P receptors [49–52] affect the development of atherosclerosis. Most but not all studies support the anti-atherogenic role of S1P. In line with this, we found atherosclerosis reduced in mice with the endothelium-specific overexpression of $S1P_1$ [24] or $S1P_3$ (this study). However, it is important to keep in mind, that even in the endothelium S1P and its receptors elicit several potentially anti-atherogenic effects beyond the regulation of transendothelial lipoprotein transport[53], for example on the transmigration of leukocytes and nitric oxide production [54]. Therefore, and because of the cholesterol lowering effects of both the $S1P_1$ and the $S1P_3$ knock-ins, we cannot conclude any causal link between reduced atherosclerosis and beneficially altered transendothelial lipoprotein transport. Further studies are needed to show the pathogenic relevance for the differential regulation of transendothelial LDL and HDL transport through S1P and its cognate receptors $S1P_1$ and $S1P_3$

Acknowledgements

The authors thank Silvija Radosavljevic and Cornelia Richter-Elsenheimer for lipoprotein isolation and excellent technical assistance. The graphical abstract was prepared with Biorender.com

Sources of Funding

This work was supported by grants from the Swiss National Science Foundation (31003A-160216 and 310030_166391/1), the 7th Framework Program of the European Commission (Project Transcard 603091), and the Systems X Program Grant MRD 2014/267 to A.v.E; from Deutsche Forschungsgemeinschaft (DFG) Grant NO406/3-1, Intramural resources of the Center for Laboratory Medicine to J.-R.N., from FIRB-IDEAS grant RBID08777T from the Italian Ministry of Education, University and Research to J.-R.N. and M.S, a Young Investigators Grant GR-2011-02346974 from the Italian Ministry of Health to F. P., and from Fondation Les Mûrons to D.W.

Data availability

The data underlying this article are available in the article and in its online supplementary material.

Author contributions

A.v.E., L.R. and J.R.N. designed the study. A.v.E, J.R.N., M.Si., and D.W. obtained funding. F.P., R.F., M.Si., and J.R.N. generated and characterized the S1P3-iECKI mice. S.V., J.R., L.R., F.P., R.F., D.P., D.W., G.P. A.P., and M.Y performed the experiments. L.R., J.R.N. and A.v.E. supervised experiments. S.V., L.R., F.P., J.R.N, and A.v.E. analyzed and interpreted data. S.V. and A.v.E. wrote the first drafts of the original and revised manuscripts. All authors critically read and revised the manuscript.

Conflict of Interest

None declared

References

1. Ference BA, Ginsberg HN, Graham I, Ray KK, Packard CJ, Bruckert E, Hegele RA, Krauss RM, Raal FJ, Schunkert H, Watts GF, Borén J, Fazio S, Horton JD, Masana L, Nicholls SJ, Nordestgaard BG, Sluis B van de, Taskinen M-R, Tokgözoglu L, Landmesser U, Laufs U, Wiklund O, Stock JK, Chapman MJ, Catapano AL. Low-density lipoproteins cause atherosclerotic cardiovascular disease. 1. Evidence from genetic, epidemiologic, and clinical studies. A consensus statement from the European Atherosclerosis Society Consensus Panel. *Eur Heart J* 2017;**38**:2459–2472.

2. Borén J, Chapman MJ, Krauss RM, Packard CJ, Bentzon JF, Binder CJ, Daemen MJ, Demer LL, Hegele RA, Nicholls SJ, Nordestgaard BG, Watts GF, Bruckert E, Fazio S, Ference BA, Graham I, Horton JD, Landmesser U, Laufs U, Masana L, Pasterkamp G, Raal FJ, Ray KK, Schunkert H, Taskinen M-R, Sluis B van de, Wiklund O, Tokgozoglu L, Catapano AL, Ginsberg HN. Low-density lipoproteins cause atherosclerotic cardiovascular disease: pathophysiological, genetic, and therapeutic insights: a consensus statement from the European Atherosclerosis Society Consensus Panel. *Eur Heart J* 2020;**41**:2313–2330.

3. Borén J, Williams KJ. The central role of arterial retention of cholesterol-rich apolipoprotein-B-containing lipoproteins in the pathogenesis of atherosclerosis: a triumph of simplicity. *Curr Opin Lipidol* 2016;**27**:473–483.

4. Randolph GJ, Miller NE. Lymphatic transport of high-density lipoproteins and chylomicrons. *J Clin Invest* 2014;**124**:929–935.

5. Jang E, Robert J, Rohrer L, Eckardstein A von, Lee WL. Transendothelial transport of lipoproteins. *Atherosclerosis* 2020;**315**:111–125.

6. Vasile E, Simionescu M, Simionescu N. Visualization of the binding, endocytosis, and transcytosis of low-density lipoprotein in the arterial endothelium in situ. *J Cell Biol* 1983;**96**:1677–1689.

7. Kraehling JR, Chidlow JH, Rajagopal C, Sugiyama MG, Fowler JW, Lee MY, Zhang X, Ramírez CM, Park EJ, Tao B, Chen K, Kuruvilla L, Larriveé B, Folta-Stogniew E, Ola R, Rotllan N, Zhou W, Nagle MW, Herz J, Williams KJ, Eichmann A, Lee WL, Fernández-Hernando C, Sessa WC. Genome-wide RNAi screen reveals ALK1 mediates LDL uptake and transcytosis in endothelial cells. *Nat Commun* 2016;**7**:13516.

8. Armstrong SM, Sugiyama MG, Fung KYY, Gao Y, Wang C, Levy AS, Azizi P, Roufaiel M, Zhu S-N, Neculai D, Yin C, Bolz S-S, Seidah NG, Cybulsky MI, Heit B, Lee WL. A novel assay uncovers an unexpected role for SR-BI in LDL transcytosis. *Cardiovasc Res* 2015;**108**:268–277.

9. Ramírez CM, Zhang X, Bandyopadhyay C, Rotllan N, Sugiyama MG, Aryal B, Liu X, He S, Kraehling JR, Ulrich V, Lin CS, Velazquez H, Lasunción MA, Li G, Suárez Y, Tellides G, Swirski FK, Lee WL, Schwartz MA, Sessa WC, Fernández-Hernando C. Caveolin-1 Regulates Atherogenesis by Attenuating Low-Density Lipoprotein Transcytosis and Vascular Inflammation Independently of Endothelial Nitric Oxide Synthase Activation. *Circulation* 2019;**140**:225–239.

10. Huang L, Chambliss KL, Gao X, Yuhanna IS, Behling-Kelly E, Bergaya S, Ahmed M, Michaely P, Luby-Phelps K, Darehshouri A, Xu L, Fisher EA, Ge W-P, Mineo C, Shaul PW. SR-B1 drives endothelial cell LDL transcytosis via DOCK4 to promote atherosclerosis. *Nature* 2019;**569**:565–569.

11. Cavelier C, Ohnsorg PM, Rohrer L, Eckardstein A von. The β-chain of cell surface F(0)F(1) ATPase modulates apoA-I and HDL transcytosis through aortic endothelial cells. *Arterioscler Thromb Vasc Biol* 2012;**32**:131–139.

12. Robert J, Lehner M, Frank S, Perisa D, Eckardstein A von, Rohrer L. Interleukin 6 stimulates endothelial binding and transport of high-density lipoprotein through induction of endothelial lipase. *Arterioscler Thromb Vasc Biol* 2013;**33**:2699–2706.

13. Rohrer L, Ohnsorg PM, Lehner M, Landolt F, Rinninger F, Eckardstein A von. High-density lipoprotein transport through aortic endothelial cells involves scavenger receptor BI and ATP-binding cassette transporter G1. *Circ Res* 2009;**104**:1142–1150.

14. Lim HY, Thiam CH, Yeo KP, Bisoendial R, Hii CS, McGrath KCY, Tan KW, Heather A, Alexander JSJ, Angeli V. Lymphatic vessels are essential for the removal of cholesterol from peripheral tissues by SR-BI-mediated transport of HDL. *Cell Metab* 2013;**17**:671–684.

15. Martel C, Li W, Fulp B, Platt AM, Gautier EL, Westerterp M, Bittman R, Tall AR, Chen S-H, Thomas MJ, Kreisel D, Swartz MA, Sorci-Thomas MG, Randolph GJ. Lymphatic vasculature mediates macrophage reverse cholesterol transport in mice. *J Clin Invest* 2013;**123**:1571–1579.

16. Cartier A, Hla T. Sphingosine 1-phosphate: Lipid signaling in pathology and therapy. *Science* 2019;**366**.

17. Wang L, Dudek SM. Regulation of vascular permeability by sphingosine 1-phosphate. *Microvasc Res* 2009;**77**:39–45.

18. Wilkerson BA, Argraves KM. The role of sphingosine-1-phosphate in endothelial barrier function. *Biochim Biophys Acta* 2014;**1841**:1403–1412.

19. Xiong Y, Hla T. S1P control of endothelial integrity. *Curr Top Microbiol Immunol* 2014;**378**:85–105.

20. Christensen PM, Liu CH, Swendeman SL, Obinata H, Qvortrup K, Nielsen LB, Hla T, Lorenzo A Di, Christoffersen C. Impaired endothelial barrier function in apolipoprotein M-deficient mice is dependent on sphingosine-1-phosphate receptor 1. *FASEB J* 2016;**30**:2351–2359.

21. Mathiesen Janiurek M, Soylu-Kucharz R, Christoffersen C, Kucharz K, Lauritzen M. Apolipoprotein M-bound sphingosine-1-phosphate regulates blood-brain barrier paracellular permeability and transcytosis. *Elife* 2019;**8**.

22. Christoffersen C, Jauhiainen M, Moser M, Porse B, Ehnholm C, Boesl M, Dahlbäck B, Nielsen LB. Effect of apolipoprotein M on high density lipoprotein metabolism and atherosclerosis in low density lipoprotein receptor knock-out mice. *J Biol Chem* 2008;**283**:1839–1847.

23. Velagapudi S, Rohrer L, Poti F, Feuerborn R, Perisa D, Wang D, Panteloglou G, Potapenko A, Yalcinkaya M, Hülsmeier AJ, Hesse B, Lukasz A, Liu M, Parks JS, Christoffersen C, Stoffel M, Simoni M, Nofer J-R, Eckardstein A von. Apolipoprotein M and Sphingosine-1-Phosphate Receptor 1 Promote the Transendothelial Transport of High-Density Lipoprotein. *Arterioscler Thromb Vasc Biol* 2021;**41**:e468–e479.

24. HAVEL RJ, EDER HA, BRAGDON JH. The distribution and chemical composition of ultracentrifugally separated lipoproteins in human serum. *J Clin Invest* 1955;**34**:1345–1353.

25. Rohrer L, Cavelier C, Fuchs S, Schlüter MA, Völker W, Eckardstein A von. Binding, internalization and transport of apolipoprotein A-I by vascular endothelial cells. *Biochim Biophys Acta* 2006;**1761**:186–194.

26. Chopra S, Shankavaram U, Bylicky M, Dalo J, Scott K, Aryankalayil MJ, Coleman CN. Profiling mRNA, miRNA and lncRNA expression changes in endothelial cells in response to increasing doses of ionizing radiation. *Sci Rep* 2022;**12**:19941.

27. Ramis JM, Collart C, Smith JC. Xnrs and activin regulate distinct genes during Xenopus development: activin regulates cell division. *PLoS One* 2007;**2**:e213.

28. Meng Q, Pu L, Qi M, Li S, Sun B, Wang Y, Liu B, Li F. Laminar shear stress inhibits inflammation by activating autophagy in human aortic endothelial cells through HMGB1 nuclear translocation. *Commun Biol* 2022;**5**:425.

29. Hogan NT, Whalen MB, Stolze LK, Hadeli NK, Lam MT, Springstead JR, Glass CK, Romanoski CE. Transcriptional networks specifying homeostatic and inflammatory programs of gene expression in human aortic endothelial cells. *Elife* 2017;**6**.

30. Rippe B, Öberg CM. Counterpoint: Defending pore theory. *Perit Dial Int* 2015;**35**:9–13.

31. Flessner MF. The transport barrier in intraperitoneal therapy. *Am J Physiol Renal Physiol* 2005;**288**:F433-42.

32. Jernigan PL, Makley AT, Hoehn RS, Edwards MJ, Pritts TA. The role of sphingolipids in endothelial barrier function. *Biol Chem* 2015;**396**:681–691.

33. Feuerborn R, Besser M, Potì F, Burkhardt R, Weißen-Plenz G, Ceglarek U, Simoni M, Proia RL, Freise H, Nofer J-R. Elevating Endogenous Sphingosine-1-Phosphate (S1P) Levels Improves Endothelial Function and Ameliorates Atherosclerosis in Low Density Lipoprotein Receptor-Deficient (LDL-R-/-) Mice. *Thromb Haemost* 2018;**118**:1470–1480.

34. Ruiz M, Okada H, Dahlbäck B. HDL-associated ApoM is anti-apoptotic by delivering sphingosine 1-phosphate to S1P1 & S1P3 receptors on vascular endothelium. *Lipids Health Dis* 2017;**16**:36.

35. Velagapudi S, Yalcinkaya M, Piemontese A, Meier R, Nørrelykke SF, Perisa D, Rzepiela A, Stebler M, Stoma S, Zanoni P, Rohrer L, Eckardstein A von. VEGF-A Regulates Cellular Localization of SR-BI as Well as Transendothelial Transport of HDL but Not LDL. *Arterioscler Thromb Vasc Biol* 2017;**37**:794–803.

36. Igarashi J, Erwin PA, Dantas AP V, Chen H, Michel T. VEGF induces S1P1 receptors in endothelial cells: Implications for cross-talk between sphingolipid and growth factor receptors. *Proc Natl Acad Sci U S A* 2003;**100**:10664–10669.

37. Frey K, Rohrer L, Potapenko A, Goetze S, Eckardstein A von, Wollscheid B. Mapping the dynamic cell surface interactome of high-density lipoprotein reveals Aminopeptidase N as modulator of its endothelial uptake. *bioRxiv* 2023.

38. Frey K, Goetze S, Rohrer L, Eckardstein A von, Wollscheid B. Decoding Functional High-Density Lipoprotein Particle Surfaceome Interactions. *Int J Mol Sci* 2022;**23**.

39. Ghaffari S, Naderi Nabi F, Sugiyama MG, Lee WL. Estrogen Inhibits LDL (Low-Density Lipoprotein) Transcytosis by Human Coronary Artery Endothelial Cells via GPER (G-Protein-Coupled Estrogen Receptor) and SR-BI (Scavenger Receptor Class B Type 1). *Arterioscler Thromb Vasc Biol* 2018;**38**:2283–2294.

40. Silver DL. A carboxyl-terminal PDZ-interacting domain of scavenger receptor B, type I is essential for cell surface expression in liver. *J Biol Chem* 2002;**277**:34042–34047.

41. Zanoni P, Velagapudi S, Yalcinkaya M, Rohrer L, Eckardstein A von. Endocytosis of lipoproteins. *Atherosclerosis* 2018;**275**:273–295.

42. Kakava S, Schlumpf E, Panteloglou G, Tellenbach F, Eckardstein A von, Robert J. Brain Endothelial Cells in Contrary to the Aortic Do Not Transport but Degrade Low-Density Lipoproteins via Both LDLR and ALK1. *Cells* 2022;**11**.

43. Kurano M, Tsukamoto K, Hara M, Ohkawa R, Ikeda H, Yatomi Y. LDL receptor and ApoE are involved in the clearance of ApoM-associated sphingosine 1-phosphate. *J Biol Chem* 2015;**290**:2477–2488.

44. Lee, S, Schleer H., Park H, Jang E, Boyer M, Tao B, Gamez-Mende A, Singh A, Folta-Stogniew E, Zhang X, Qin L, Xiao Y, Xu L, Zhang J, Hu X, Pashos E, Tellides G, Shaul PW, Lee WL, Fernandez-Hernando C, Eichmann A, Sessa WC . Genetic or therapeutic neutralization of ALK1 reduces LDL transcytosis and atherosclerosis in mice. *Nat Cardiovasc Res* **2**, 438–448 (2023).

45 Potì F, Ceglarek U, Burkhardt R, Simoni M, Nofer J-R. SKI-II--a sphingosine kinase 1 inhibitor--exacerbates atherosclerosis in low-density lipoprotein receptor-deficient (LDL-R-/-) mice on high cholesterol diet. *Atherosclerosis* 2015;**240**:212–215.

46. Poti F, Bot M, Costa S, Bergonzini V, Maines L, Varga G, Freise H, Robenek H, Simoni M, Nofer J-R. Sphingosine kinase inhibition exerts both pro- and anti-atherogenic effects in low-density lipoprotein receptor-deficient (LDL-R(-/-)) mice. *Thromb Haemost* 2012;**107**:552–561.

47. Bot M, Veldhoven PP Van, Jager SCA de, Johnson J, Nijstad N, Santbrink PJ Van, Westra MM, Hoeven G Van Der, Gijbels MJ, Müller-Tidow C, Varga G, Tietge UJF, Kuiper J, Berkel TJC Van, Nofer J-R, Bot I, Biessen EAL. Hematopoietic sphingosine 1-phosphate lyase deficiency decreases atherosclerotic lesion development in LDL-receptor deficient mice. *PLoS One* 2013;**8**:e63360.

48. Bosteen MH, Madsen Svarrer EM, Bisgaard LS, Martinussen T, Madsen M, Nielsen LB, Christoffersen C, Pedersen TX. Effects of apolipoprotein M in uremic atherosclerosis. *Atherosclerosis* 2017;**265**:93–101.

49. Potì F, Gualtieri F, Sacchi S, Weißen-Plenz G, Varga G, Brodde M, Weber C, Simoni M, Nofer J-R. KRP-203, sphingosine 1-phosphate receptor type 1 agonist, ameliorates atherosclerosis in LDL-R-/- mice. *Arterioscler Thromb Vasc Biol* 2013;**33**:1505–1512.

50. Poti F, Costa S, Bergonzini V, Galletti M, Pignatti E, Weber C, Simoni M, Nofer J-R. Effect of sphingosine 1-phosphate (S1P) receptor agonists FTY720 and CYM5442 on atherosclerosis development in LDL receptor deficient (LDL-R$^{-/-}$) mice. *Vascul Pharmacol* 2012;**57**:56–64.

51. Skoura A, Michaud J, Im D-S, Thangada S, Xiong Y, Smith JD, Hla T. Sphingosine-1-phosphate receptor-2 function in myeloid cells regulates vascular inflammation and atherosclerosis. *Arterioscler Thromb Vasc Biol* 2011;**31**:81–85.

52. Keul P, Tölle M, Lucke S, Wnuck Lipinski K von, Heusch G, Schuchardt M, Giet M van der, Levkau B. The sphingosine-1-phosphate analogue FTY720 reduces atherosclerosis in apolipoprotein E-deficient mice. *Arterioscler Thromb Vasc Biol* 2007;**27**:607–613.

53. Galvani S, Sanson M, Blaho VA, Swendeman SL, Obinata H, Conger H, Dahlbäck B, Kono M, Proia RL, Smith JD, Hla T. HDL-bound sphingosine 1-phosphate acts as a biased agonist for the endothelial cell receptor S1P1 to limit vascular inflammation. *Sci Signal* 2015;**8**:ra79.

54. Potì F, Simoni M, Nofer J-R. Atheroprotective role of high-density lipoprotein (HDL)-associated sphingosine-1-phosphate (S1P). *Cardiovasc Res* 2014;**103**:395–404.

Legends to the figures

Figure 1: Targeting vector/transgene structure and Cre-mediated activation of transcription and demonstration of $S1P_3$ in the endothelium of aortas from Apoe haploinsufficient mice without (CTRL) or with overexpression of $S1P_3$ ($S1P_3$-iECKI). **(a)** The transgene, inserted within the ROSA26 locus via homologous recombination, contains the murine S1pr3 cDNA, separated from the synthetic cytomegalovirus early enhancer/chicken β-actin (CAG) strong promoter by a LoxP-STOP-Neomicin-LoxP (LSL) cassette. S1pr3LSL mice were crossed with the tamoxifen inducible Apoe-/-Cdh5-CreERT2 mice, which express the Cre recombinase under control of the VE-cadherin promoter, active in endothelial cells only. Gene overexpression was achieved by intraperitoneal injection of tamoxifen and the LSL insert is hence excised only in Cre-expressing cells $S1P_3$-iECKI: $S1P_3$-inducible endothelial cell knock-in (mice). **(b)** Agarose gel electrophoresis of PCR-amplified genomic DNA from lungs of wild type mice and $S1P_3$-ECKI mice. From the left: lane 1 molecular weight marker (Marker XIV, Roche); lanes 2 through 19, eighteen samples of mouse genomic DNA; lane 20 water. Upper bands (≈450bp) in samples depicted in lanes 2,3, 8, 9,11,12, 13,14,15,17, 18 and 19 identify samples of $S1P_3$ ECKI mice with the excision event. **(c-f)** Figure shows en-face prepared aortas immunostainings. Aortas were quickly cleared from the adventitial tissue, opened longitudinally and incubated with primary and secondary antibodies conjugated with green or red fluorescent dyes, as indicated. Nuclei were counterstained with DAPI. Images were captured by confocal microscope and z-axis projections of 14 scanned planes are shown. Scale bar = 10μm. Original micrographs are shown as supplementary figure 1. **(d, f)** Orthogonal projections of single optical slices from z-stack. For each image, right side and bottom side rectangles (the projections) clearly show the correspondence of the immunofluorescence signal with the endothelial lining. This view mode highlights also the localization of $S1P_3$ receptors at the membrane level (red and green signals overlap generating orange and yellow signals).

Figure 2: $S1P_3$ agonist has opposite effects on transendothelial transport association and binding, of HDL and LDL in HAECs. HAECs were cultured for 72hours. Cells were then treated with 100nM CYM5541 for 30minutes at 37 ºC. . For the measurement of transport, HAECs were cultured on inserts. The transport of 10μg/mL ^{125}I-HDL (**a**) or10μg/mL ^{125}I-LDL (**b**) from the apical to basolateral compartment was measured after 1 hour incubation at 37 ºC. To study cellular binding and association, HAECs were incubated with 10μg/mL of ^{125}I-HDL or ^{125}I-LDL for 1hour in the absence (total) or in the presence of 40-fold excess of unlabeled HDL and LDL, respectively, to record unspecific interactions. Specific binding and association were calculated by subtracting unspecific values from total values. To measure specific cell association, cells were incubated with

^{125}I-HDL (**c**) or ^{125}I-LDL (**d**) at 37 ºC The results are represented as means±SEM of four independent triplicate experiments (n=4). **+++***P*≤ 0.001, **++***P*≤ 0.01, **+***P*≤ 0.05 (two-tailed Student's *t*-test) .

Figure 3: S1P$_3$ inhibition has opposite effects on transendothelial transport , association and binding of HDL and LDL in HAECs HAECs were cultured for 72hours. Cells were then treated with 110nM TY52156 for 30minutes at 37 ºC. For the measurement of transport, HAECs were cultured on inserts. The transport of 10µg/mL ^{125}I-HDL (**a**) or10µg/mL ^{125}I-LDL (**d**) from the apical to basolateral compartment was measured after 1 hour incubation at 37 ºC. To study cellular association and binding, HAECs were incubated with 10µg/mL of ^{125}I-HDL (**b,c**) or ^{125}I-LDL (**e,f**) for 1hour at 37ºC and 4ºC, respectively, in the absence (total) or in the presence of 40-fold excess of unlabeled HDL and LDL, respectively, to record unspecific interactions. Specific association (**b,e**) and binding (**c,f**), were calculated by subtracting unspecific values from total values. The results are represented as means±SEM of four independent triplicate experiments (n=4). **+++***P*≤ 0.001, **++***P*≤ 0.01, **+***P*≤ 0.05, n.s represents "not significant" (two-tailed Student's *t*-test).

Figure 4: RNA interference with S1P$_3$ counteracts the effects of CYM5541 on the association of HDL and LDL with HAECs To study specificity of S1P$_3$ agonist treatment on the cellular association of ^{125}I-HDL and ^{125}I-LDL, HAECs were transfected with a specific siRNA against S1PR3 or with non-silencing control siRNA (NS control) and cellular association assays were performed 72hours post-transfection. Cells were then treated with 100nM CYM5541 for 30minutes, at 37 ºC. Cellular association of (**a**) ^{125}I-HDL and (**b**) ^{125}I-LDL were measured at 37 ºC by pre-treating cells with the S1P$_3$ agonist. The results are represented as means±SEM of three independent triplicate experiments (n=3). **+++***P*≤ 0.001 (Kruskal-Wallis one-way ANOVA followed by Student-Newman-Keuls post hoc test).

Figure 5: S1P$_3$ agonists modulate SR-BI dependent binding, association and transport of HDL by HAECs. To study cellular binding, association and transport of ^{125}I-HDL, HAECs were transfected with a specific siRNA against SR-BI or with non-silencing control siRNA (NS control) and assays were performed 72hours post-transfection. Cells were then treated with 100nM CYM5541 for 30minutes, at 37 ºC. (**a**) cellular binding of ^{125}I-HDL was measured at 4 ºC by pre-treating cells with the S1P$_3$ agonist. (**b**) cellular association of ^{125}I-HDL was measured at 37 ºC by pre-treating cells with the S1P$_3$ agonist. (**c**) for the measurement of transport of ^{125}I-HDL, HAECs were cultured on inserts. The transport of ^{125}I-HDL was measured by pre-treatment with the S1P$_3$ agonist from the apical to basolateral compartment was measured at 37 ºC. The results are represented as means±SEM of four independent triplicate experiments (n=4). **+++***P*≤ 0.001, **++***P*≤

0.01, +$P \leq 0.05$ (Kruskal-Wallis one-way ANOVA followed by Student-Newman-Keuls post hoc test).

Figure 6: Effects of $S1P_3$ on the expression of SR-BI . a and b): Short term pharmacological activation of $S1P_3$ increases the cell surface expression of SR-BI. HAECs were cultured for 72hours. Cells were then treated with 100nM CYM5541 or 110 nM TY52156 for 30minutes at 37 ºC. Cell surface expression of SR-BI in HAECs was measured using Western blot analysis in total cell lysates (left) and on the cell surface (right) (**a**). The western blots were probed with anti-SR-BI and anti-TBP (used as a control for intracellular protein expression). (**b**) shows the summary of four independent experiments quantified by densitometry. ++$P \leq 0.01$ (two-tailed Student's *t*-test). (**c and d)Knock-downs of *S1P1* or *S1P3* dramatically decrease both SR-B1 protein and *SCARB1* mRNA expression.** HAECs were seeded at a density of 0.4×10^6 cells/well in 6-well plates. The cells were reverse transfected with siRNA (10 nM) targeted to *SCARB1, S1P1 or S1P3*, or with non-silencing control siRNA (NC siRNA) for 72 h. The expression of SR-B1 protein and *SCARB1* mRNA was determined by western blot analyses and qRT-PCR, respectively. TATA-binding protein (TBP) and GAPDH mRNA were used as the internal control for western blot analyses and RT-qPCR, respectively. **f) Increased endothelial SR-BI expression in the aorta of S1P3-iECKI mice .** Figures show en-face prepared aortic immunostainings of SR-BI in the endothelium of aortas from Apoe haploinsufficient mice without (CTRL: upper part) or with overexpression of S1P3 (lower panel). Aortas were quickly cleaned of adventitial tissue, opened longitudinally and incubated with primary and secondary antibodies conjugated with green or red fluorescent dyes, as indicated. Nuclei were counterstained with DAPI. Images were captured by confocal microscope and z-axis projections of 14 scanned planes are shown. Scale bar = 10µm. Original micrographs are shown as supplementary figure 9.

Figure 7: $S1P_3$ regulates transendothelial transport of LDL independently of LDLR, SR-BI and ACVRL1 in HAECs. HAECs were transfected with a specific siRNA against *LDLR* or *SCARB1* or *ACVRL1* or with non-silencing control siRNA (NS control) and assays were performed 72hours post-transfection. Cells were then treated with 110nM TY52156 for 30minutes at 37 ºC. (**a**) cellular binding of ^{125}I-LDL was measured at 4 ºC by pre-treating cells with the $S1P_3$ inhibitor. (**b**) cellular association of ^{125}I-LDL was measured at 37 ºC. (**c**) for the measurement of transport of ^{125}I-LDL, HAECs were cultured on inserts. After pre-treatment with the $S1P_3$ inhibitor, the transport of ^{125}I-LDL from the apical to basolateral compartment was measured at 37 ºC. The results are represented as means±SEM of three independent triplicate experiments (n=3). Vehicle control represents DMSO treated condition. +++P≤ 0.001, ++P≤ 0.01, +P≤ 0.05 ; ***P≤ 0.001, **P≤ 0.01,

*P≤ 0.05, n.s represents “not significant” (Kruskal-Wallis one-way ANOVA followed by Student-Newman-Keuls post hoc test).

Table 1

Dye	CTRL	$S1P_3$-KI
Evans' Blue (arbU)	0.13 +/- 0.01	0.11 +/- 0.02
Fluorescent LDL (arbU)	89.0 +/- 2.9	45.3 +/- 4.7*
Flurorescent HDL (arbU)	18.5 +/- 5.2	27.5 +/- 2.9*

Table 1: Endothelium-specific overexpression of $S1P_3$ differentially regulates endothelial permeability for LDL, HDL, and Evan's Blue in Apoe haploinsufficient mice Intravenous (i.v) injection of Evan's Blue or DyLight-LDL or DyLight-HDL and i. p. stimulation with LPS.Collection of peritoneal fluid after 120 minutes. (N = 3 - 4 per group; *: $P < 0.05$, one-way ANOVA followed by Student-Newman-Keuls post-hoc test)

Figure 1

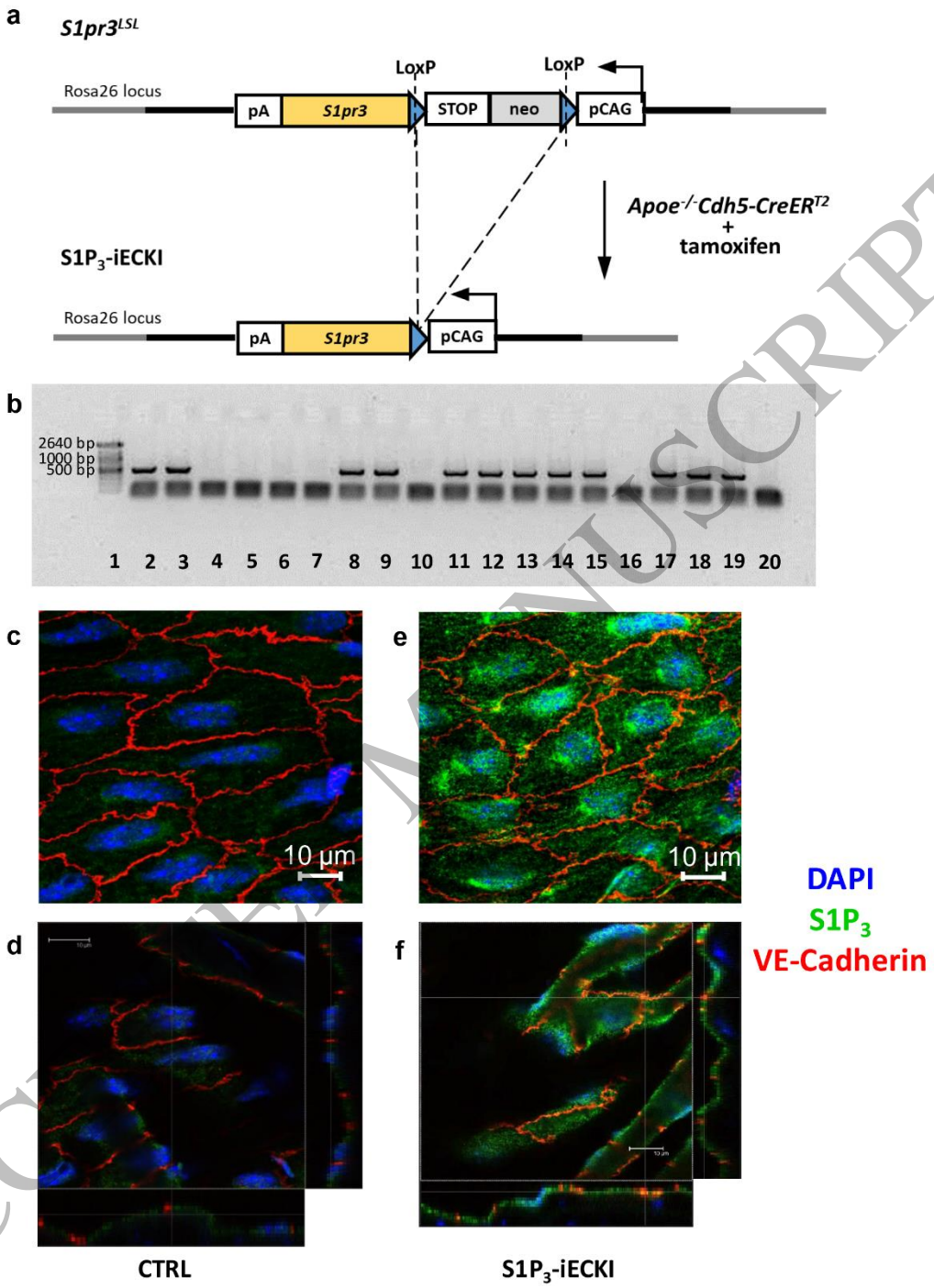

Figure 1
170x246 mm (x DPI)

Figure 2

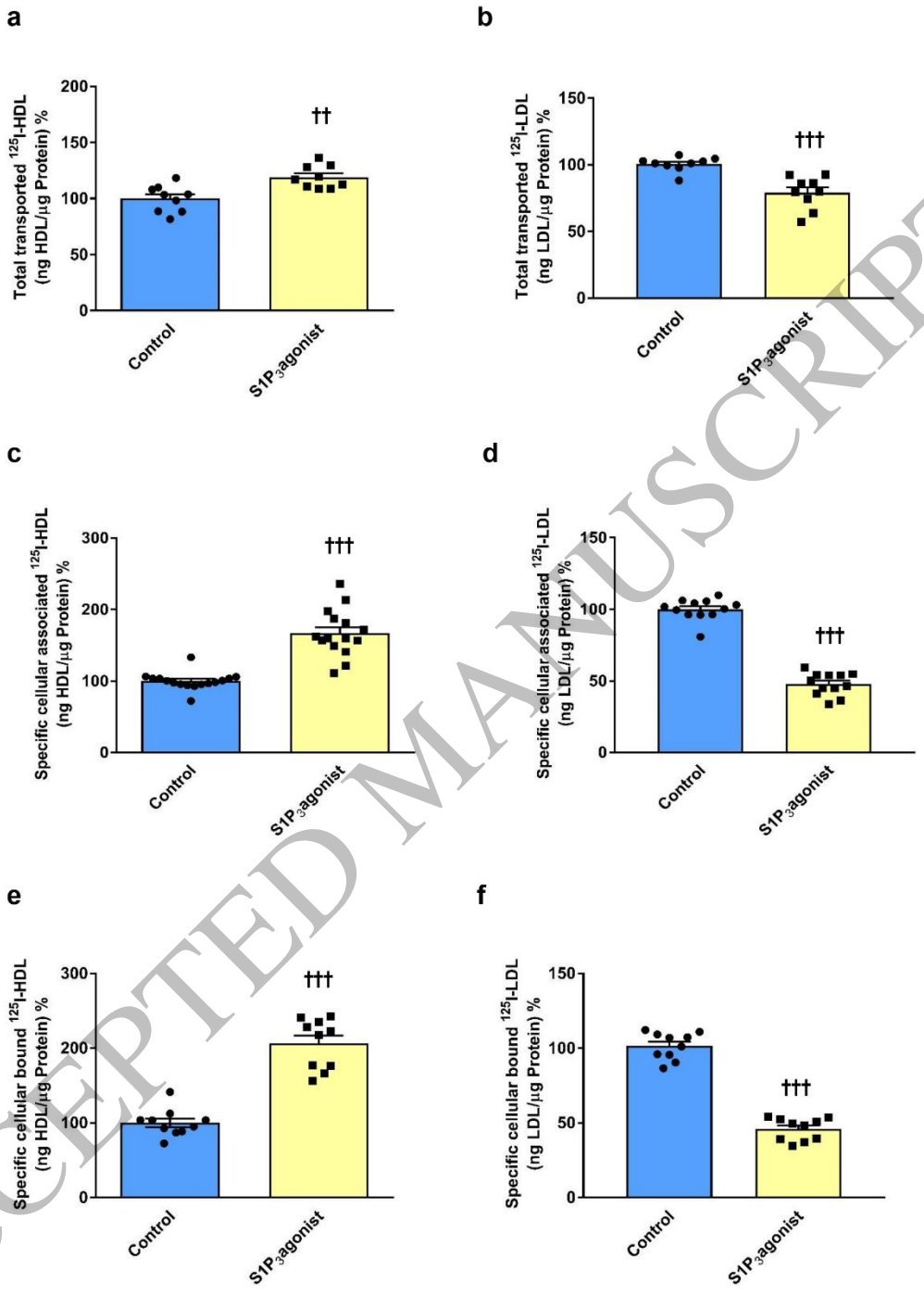

Figure 2
170x246 mm (x DPI)

Figure 3

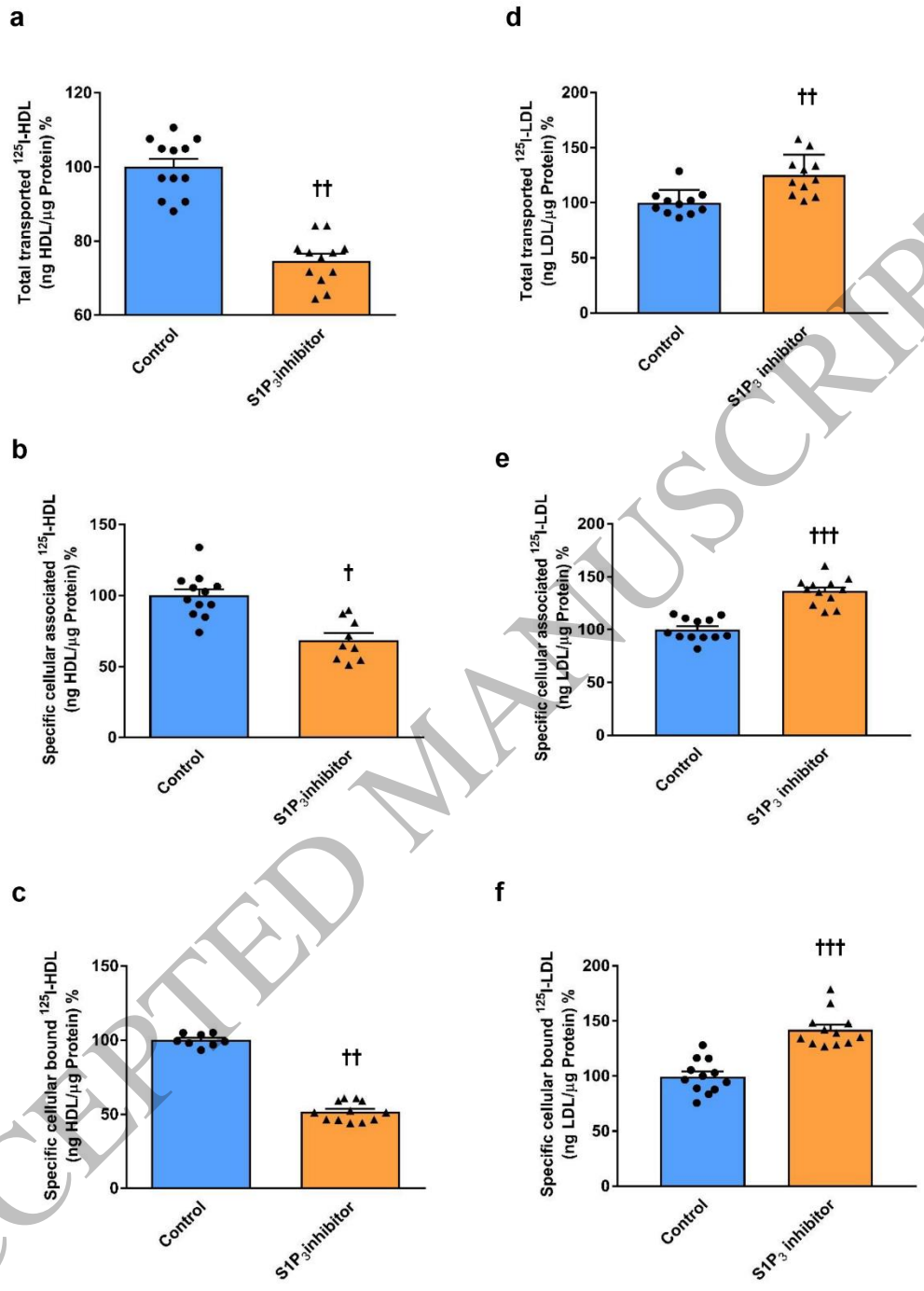

Figure 3
170x246 mm (x DPI)

Figure 4

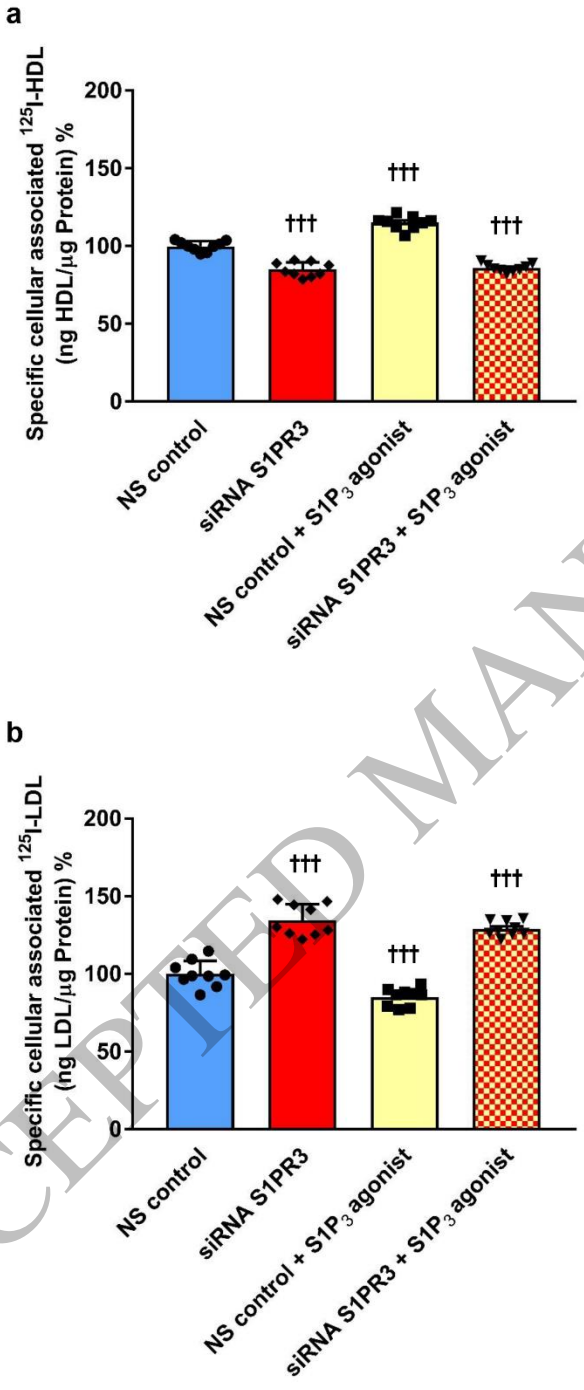

Figure 4
170x246 mm (x DPI)

Figure 5

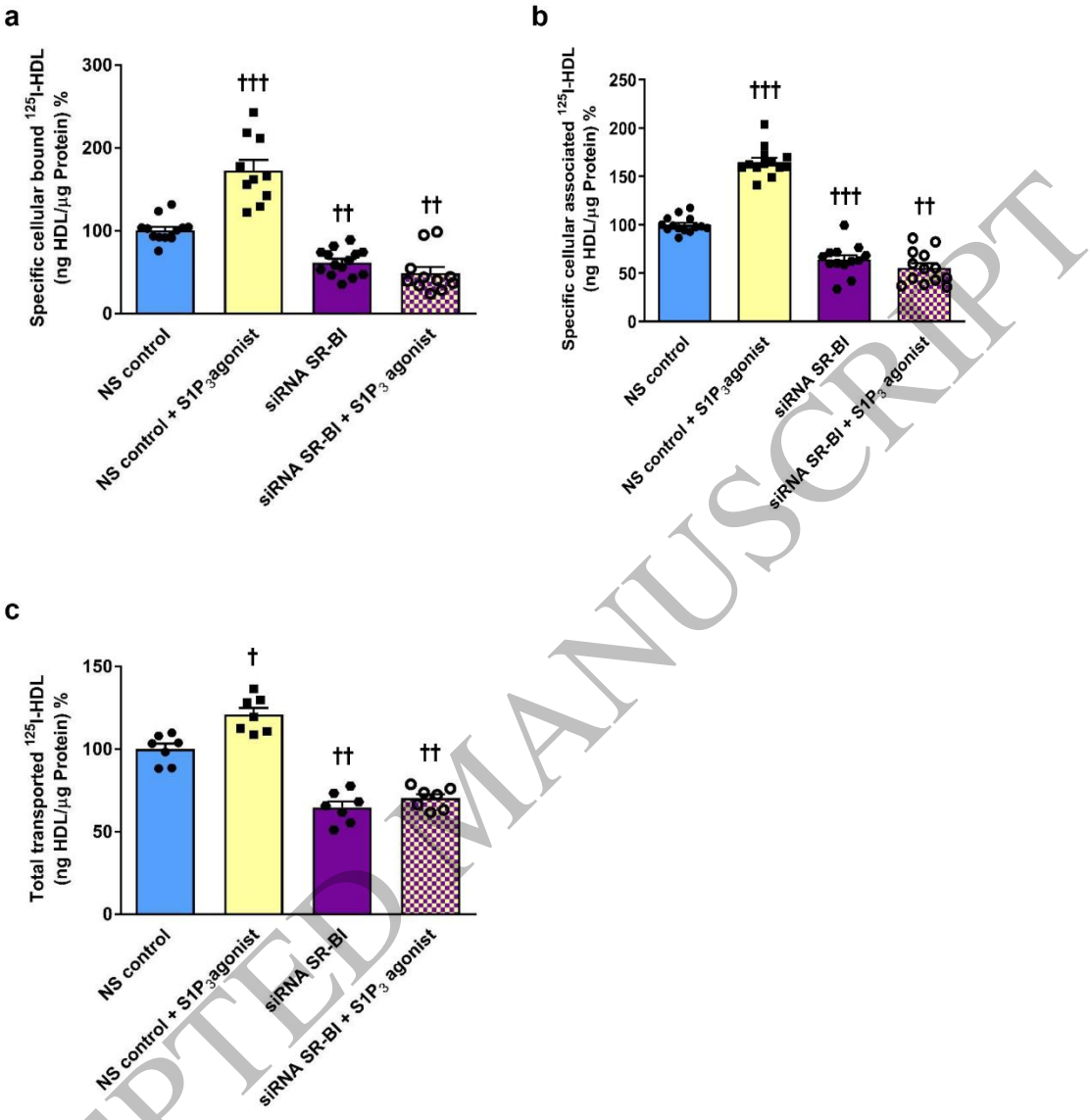

Figure 5
170x246 mm (x DPI)

Figure 6

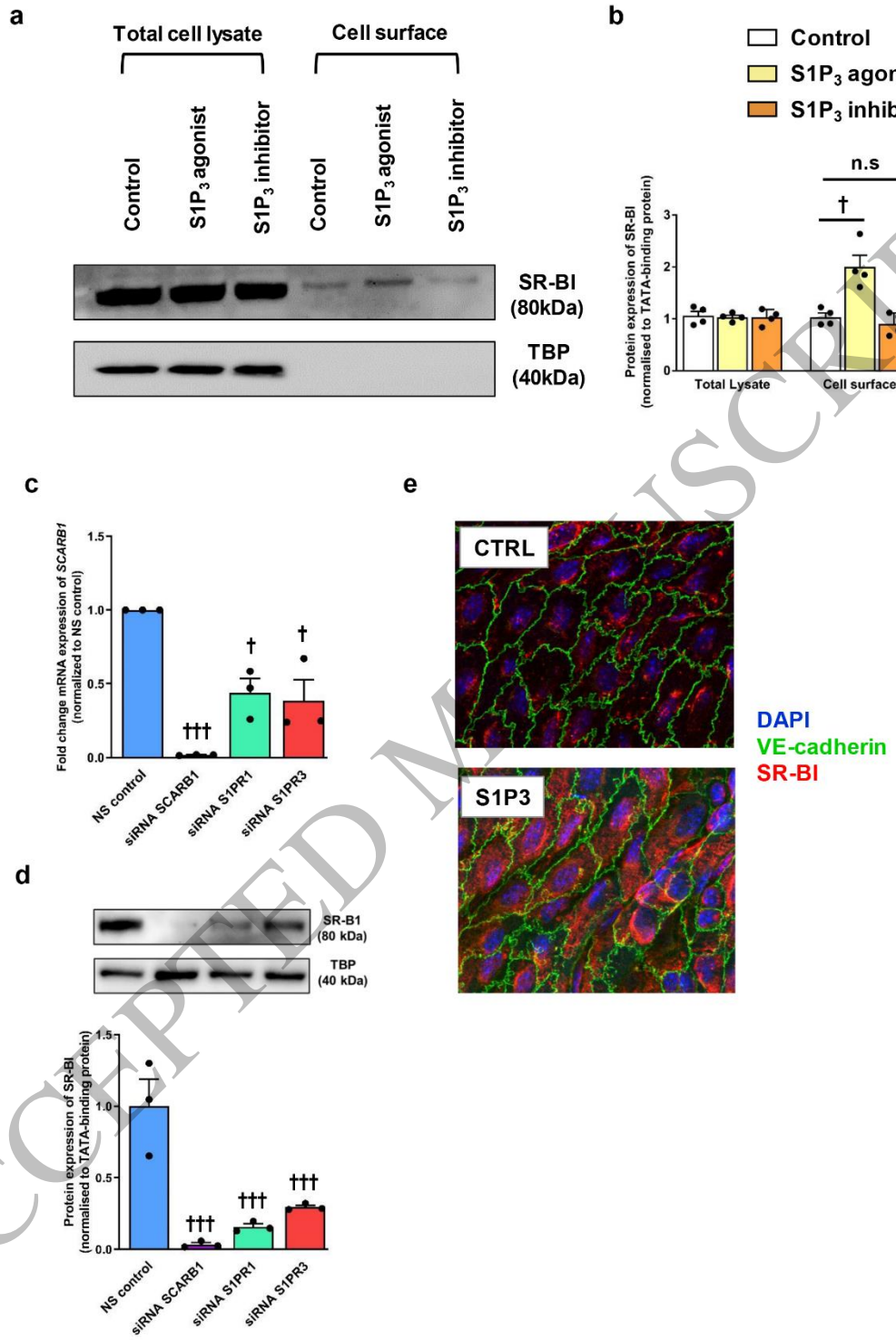

Figure 6
170x246 mm (x DPI)

Figure 7

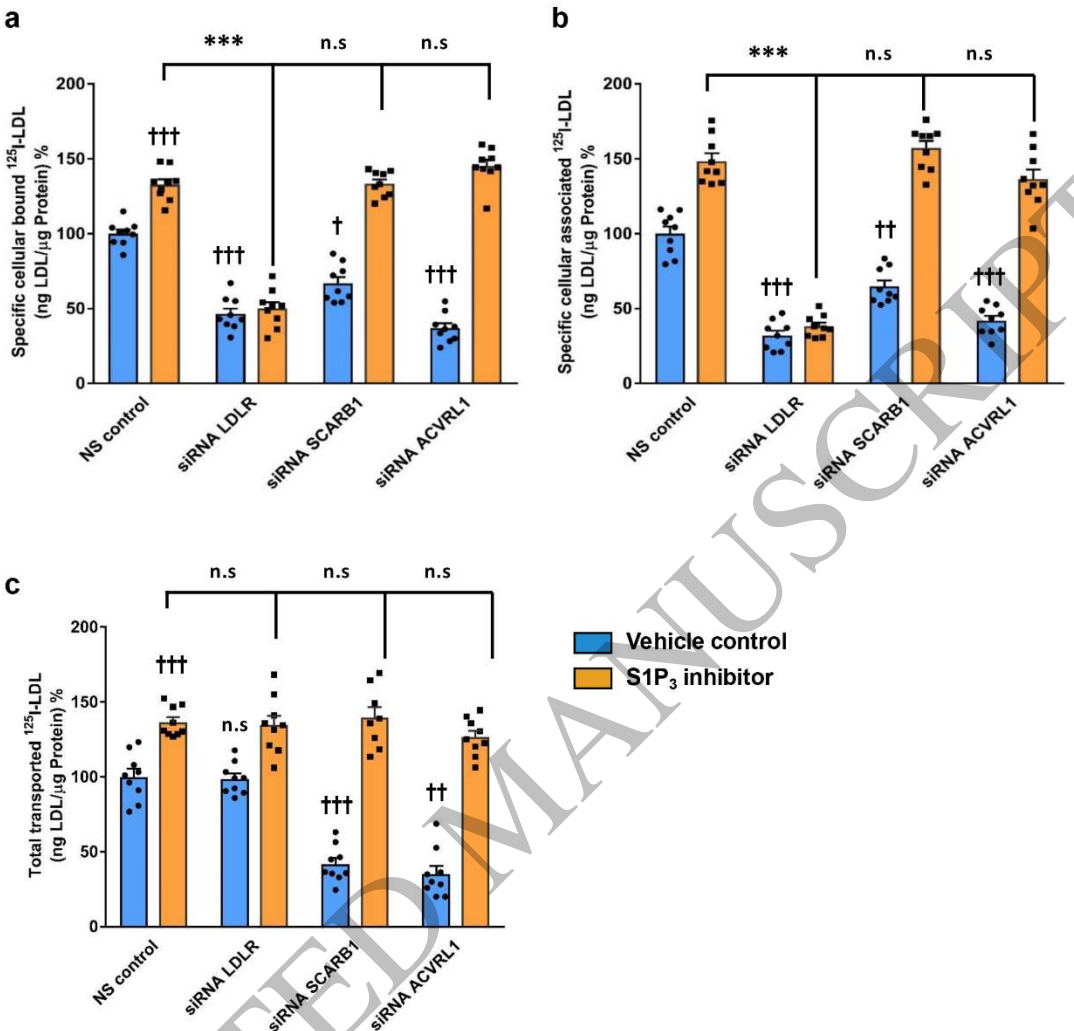

Figure 7
170x246 mm (x DPI)

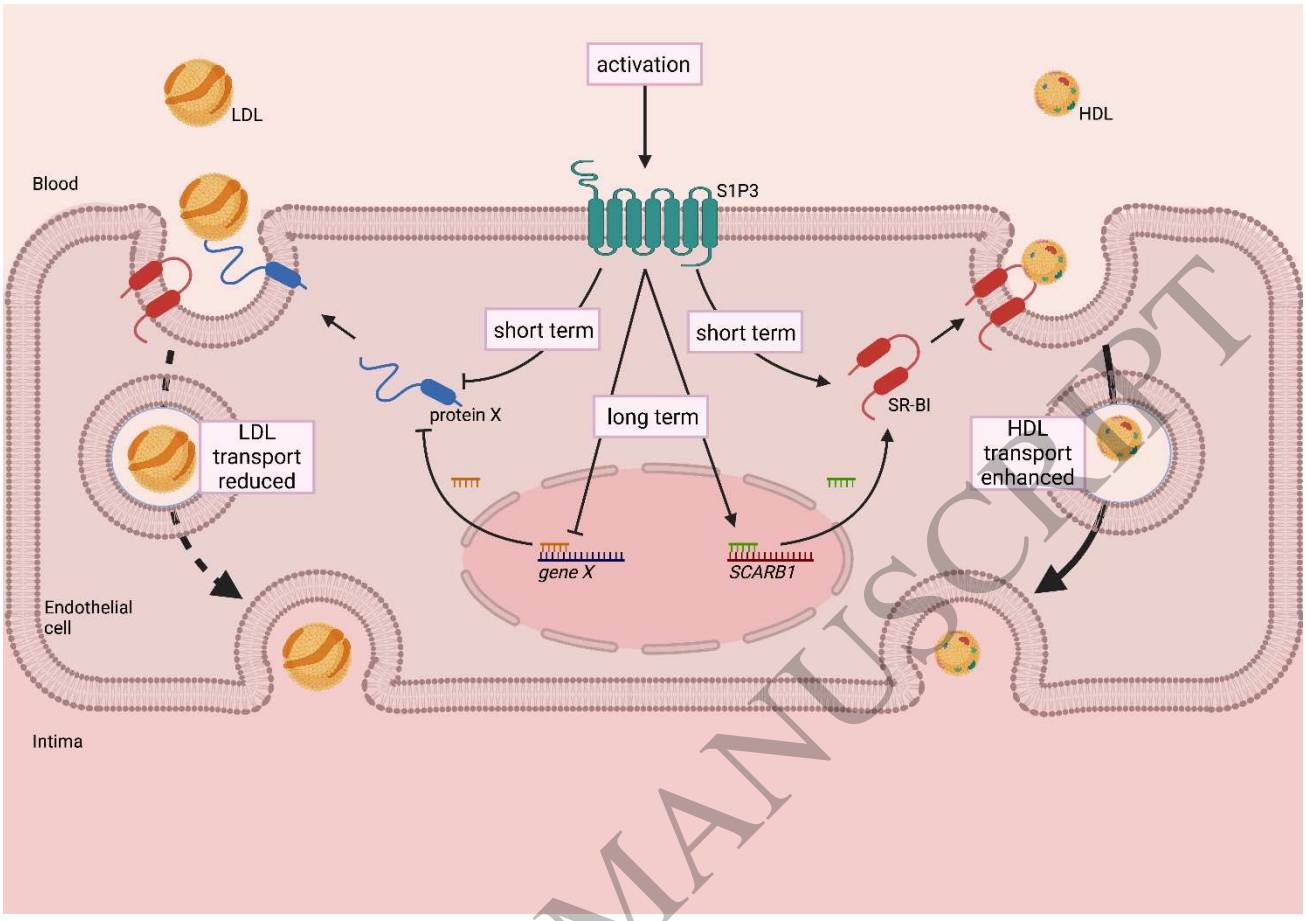

Graphical Abstract